Ultraviolet spectral properties of magellanic and non-magellanic irregulars, H II and starburst galaxies[*]

C. Bonatto[1], **E. Bica**[1], **M.G. Pastoriza**[1], and **D. Alloin**[2,3]

[1] Universidade Federal do Rio Grande do Sul, IF, CP 15051, Porto Alegre 91501–970, RS, Brazil
[2] SAp CE-Saclay, Orme des Merisiers Bât 709, F-91191 Gif-Sur-Yvette Cedex, France

Abstract. This paper presents the results of a stellar population analysis performed on nearby ($V_R \leq 5\,000$ km s^{-1}) star-forming galaxies, comprising magellanic and non-magellanic irregulars, H II and starburst galaxies observed with the IUE satellite. Before any comparison of galaxy spectra, we have formed subsets according to absolute magnitude and morphological classification. Subsequently, we have coadded the spectra within each subset into groups of similar spectral properties in the UV. As a consequence, high signal-to-noise ratio templates have been obtained, and information on spectral features can now be extracted and analysed. Seven groups resulted from this procedure: the magellanic irregulars (including H II galaxies) produced two different blue spectral groups; the non-magellanic irregulars could be grouped into two spectral groups with rather peculiar properties; and the luminous starbursts produced one flat and two blue template spectra. Their stellar populations are analysed by means of a population synthesis algorithm based on star cluster spectral components. The synthetic spectra reproduce the observed ones successfully (except the non-magellanic irregular groups) both in terms of continuum distribution and spectral features. The synthesis flux fractions of different age groups were transformed into mass fractions, allowing inferences on the star formation histories. Young stellar populations (age < 500 Myrs) are the main flux contributors; in a few cases the intermediate age population (age$\approx$ 1–2 Myrs) is important, while the old bulge population contributes at most with ≈ 2 % of the $\lambda 2646$ Å flux in the case of starburst galaxies, and is negligible in the magellanic irregulars. We also study the reddening values and the extinction law: an SMC-like extinction law is appropriate for all cases.

Key words: galaxies: compact – galaxies: irregular – galaxies: starbust – galaxies: stellar content – ultraviolet: galaxies

1. Introduction

Following our systematic study of galaxy spectra available in the International Ultraviolet Explorer (IUE) Satellite library,

we dedicate the present work to galaxy types with enhanced star formation in the nearby Universe ($V_R \leq 5\,000$ kms^{-1}). We include low and moderate luminosity irregular galaxies (magellanic and non-magellanic irregulars, and H II galaxies) and high-luminosity ones (mergers, disrupting, etc.). The same method used in the analyses of star clusters, early-type and spiral galaxies (Bonatto et al. 1995, 1996 and 1998, hereafter referred to as Papers I, II and III, respectively), i.e. that of grouping objects with similar spectra into templates of high signal-to-noise (S/N) ratio, is now applied to the sample of irregular and/or peculiar galaxies.

Among the spectral studies on irregulars carried out with IUE data, we recall that several H II and irregular galaxies were presented in the IUE UV catalogue of extragalactic H II regions (Rosa et al. 1984). More recently, irregulars and H II galaxies, as well as luminous starbursts, were included in the IUE atlas of star-forming galaxies (Kinney et al. 1993), and their spectral properties discussed, in conjunction with other spectral ranges, by Storchi-Bergmann et al. (1995).

By grouping spectra of similar properties it is possible to obtain unprecedented high (S/N) ratio galaxy templates. For the interpretation of the groups obtained in this work we make use of the population synthesis algorithm of Bica (1988), which was recently adapted to the UV range in a paper dealing with the analysis of IUE spectra of spiral galaxies (Paper III). The base elements are the single-aged UV templates of stellar populations, i.e. the star cluster spectral groups from Paper I. In the synthesis procedure we test different reddening laws for the UV, including the Galactic, LMC and SMC ones (Papers II and III).

In Sect. 2 we present the IUE sample of irregular, H II and starburst galaxies. In Sect. 3 the objects are grouped according to spectral similarities. Equivalent width and continuum measurements, are presented in Sect. 4, where we also discuss their relation with global properties. The stellar population is analysed and discussed in Sect. 5. In Sect. 6 we discuss the nature of the emission lines. Finally, the conclusions of this work are given in Sect. 7.

2. Data set

The data have been obtained from the Space Telescope Science Institute archives and correspond to the *IUE New Spectral Image*
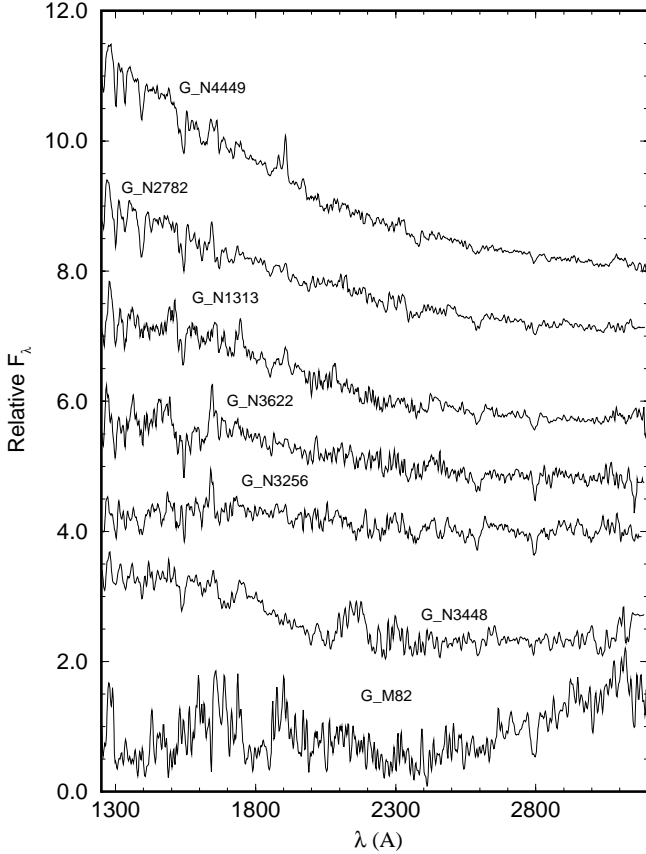

Fig. 1. Nearby irregular and starburst galaxy groups (see Table 1). Flux in F_λ units, normalised at $\lambda 2646$ Å. Constants have been added to the spectra for clarity purposes, except for the bottom one.

Fig. 2. Comparison of global properties of our groups with absolute magnitude. In the top panel we show the $12\,\mu$m luminosity, and the remaining ones deal with equivalent widths of strong absorption features in the UV. Notice that in most cases we are dealing with upper limits in $L_{12\mu}$m.

Processing System (NEWSIPS) re-processed spectra. We have selected the available SWP, LWP and LWR spectra of nearby ($V_R \leq 5\,000\,\mathrm{km\,s^{-1}}$) magellanic and non-magellanic irregulars, those classified as Blue Compact galaxies/H II galaxies, as well as luminous galaxies with different sorts of morphological peculiarities such as mergers, interacting galaxies, highly disturbed galaxies, etc, i.e. all those types related to possibly enhanced star formation. We consider here only the spectra obtained in the large aperture ($10'' \times 20''$) mode. In Table 1 we present the objects used in this study along with some relevant data obtained mainly from de Vaucouleurs et al. 1991 (hereafter RC3) and the NASA/IPAC Extragalactic Database (NED)[1]. We have gathered in Table 1 the following information on the sample galaxies, by columns: (1) different identifications; (2) PGC number; (3) morphological type (T); (4) foreground absorption A_B; (5) total blue magnitude B_T; (6) M_B assuming $H_O = 75\,\mathrm{km\,s^{-1}\,Mpc^{-1}}$; (7) $12\,\mu$m luminosity obtained from IRAS fluxes given in NED; (8) heliocentric radial velocity, and (9) complementary remarks. Absolute magnitudes M_B were calculated using Galactic Standard of Rest (V_G) velocities (RC3), while optical and H I heliocentric veloc-

ities (V_R) were considered for redshift corrections in the IUE spectra. The A_B values were used to correct all spectra for the foreground (Galactic) reddening using Seaton's (1979) law and $A_B/E(B-V) = 4.0$. Thus, in the subsequent analyses all spectra are corrected for the *foreground reddening and redshift.*

3. Galaxy spectral groups

Galaxies exhibit a wide range of spectral properties, but those presenting similarities can be grouped, a procedure which allows one to study their average properties in more detail, from data with an improved (S/N) ratio. In order to obtain such data and to analyse the UV spectral lines it is necessary first to coadd the available IUE spectra of each individual object, and subsequently to coadd into a spectral group the spectra of objects which show close similarities. In the present grouping procedure the ultimate criterion is the similarity of the UV spectra at the available (S/N) ratio. However, we also consider the spectral properties in the visible and near-IR ranges found in the literature, together with the classifications as H II galaxy, starburst or usual normal stellar population types. For more details on the grouping procedure see Papers I, II and III.

In Table 2 we present the resulting groups with the galaxies they are made of, along with the number of SWP and LWP/LWR

---

[1] The NASA/IPAC Extragalactic Database (NED) is operated by the Jet Propulsion Laboratory, California Institute of Technology, under contract with the National Aeronautics and Space Administration.
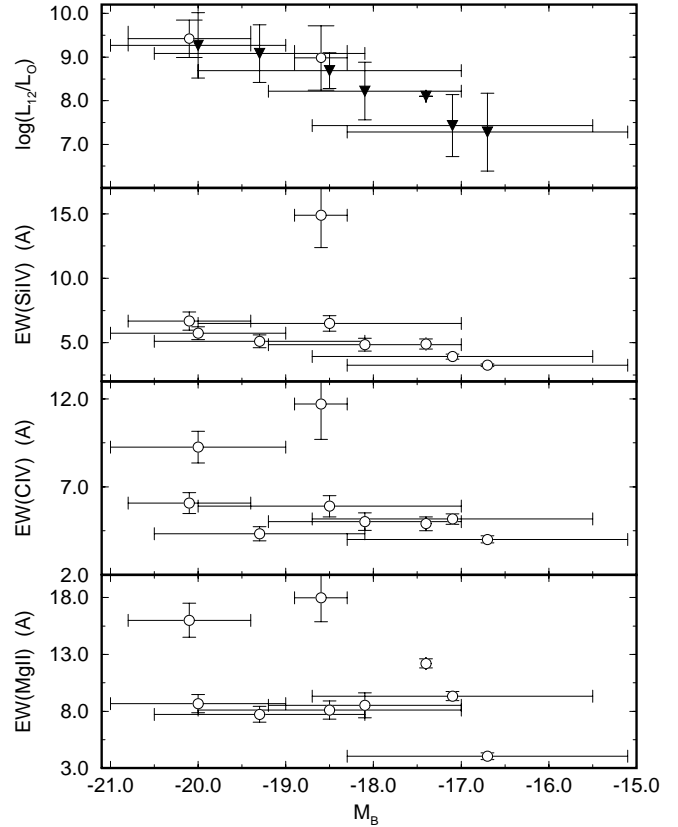
Table 1. Nearby irregular galaxies

Group/Object	PGC #	T	A_B mag	B_T mag	M_B mag	$\log\left(\frac{L_{12}}{L_\odot}\right)$	V_R km s^{-1}	Remarks
G_N1313 – Sm/Im and H II *galaxies with blue spectra*								
ESO 435-IG20, TOL 0957-278, AM 0957-275	28863		0.18	14.18	-17.1	—	1246	in system, pec, BCG
IC 3017, CGCG 69- 64, VCC 10	38627		0.01	15.12	-16.9	—	1914	
Mrk 33, Haro 2, UGC 5720, ARP 233	35856	10.0	0.00	13.38	-17.9	8.49	1377	BCG
Mrk 67, UGC A 372	48501		0.00	16.70	-14.1	<7.78	1080	
Mrk 450, UGC 8323, MCG +06-29-065	46065	10.0	0.00	14.56	-15.6	<7.51	804	
Mrk 487, UGC A410, I Zw 123	55616		0.02	15.45	-14.2	<7.27	625	BCDG
NGC 625, ESO 297-G5, IRAS 01329-4141	5896	9.0	0.03	11.21	-17.4	7.35	383	
NGC 1313, ESO 82-G11, VV 436	12286	7.0	0.04	9.29	-19.6	8.14	446	
NGC 1569, UGC 3056, VII Zw 16, ARP 210	15345	10.0	2.18	9.42	-17.8	6.52	-200	
NGC 1800, ESO 422-G30, IRAS 05045-3201	16745	10.0	0.00	12.87	-17.1	<7.49	744	in pair
NGC 2537, Mrk 86, UGC 4274, ARP 6	23040	9.0	0.16	12.02	-17.0	7.33	444	in pair, BCDG
NGC 3353, Mrk 35, UGC 5860, Haro 3	32103	3.0	0.00	13.00	-17.5	8.25	935	BCDG, Im?
NGC 3396, UGC 5935, in ARP 270	32434	10.0	0.00	12.32	-19.4	—	1667	in pair
NGC 3432, UGC 5986, ARP 206	32774	9.0	0.00	11.03	-18.6	7.88	629	
NGC 5204, UGC 8490, IRAS 13277+5840	47368	9.0	0.00	11.48	-17.0	<6.96	202	
NGC 5474, UGC 9013	50216	6.0	0.00	11.30	-17.9	<7.24	230	
NGC 6822, MCG -02-50-006, DDO 209	63616	10.0	0.93	8.38	-16.5	5.57	-26	
NGC 7250, Mrk 907, UGC 11980	68535	8.0	0.67	12.08	-19.3	7.98	1165	
UGC 6456, VII Zw 403, MCG +13-08-058	35286	99.0	0.10	14.50	-14.6	7.14	-49	pec, multiple?, BCDG
UGC 8315N, MCG +07-27-052	46017		0.00	15.20	-15.8	—	1164	in double system
G_N4449 – Sm/Im and H II *galaxies with very blue spectra*								
Holmberg II, MCG +12-08-033, UGC 4305	23324	10.0	0.10	10.85	-16.8	<6.62	157	in M 81 group
IC 1613, UGC 668, DDO 8	3844	10.0	0.02	9.82	-15.2	<5.39	-237	
IC 2458, Mrk 108, MCG +11-12-005, VII Zw 276	26485	90.0	0.16	15.10	-16.5	—	1437	in pair, BCDG
IC 2574, UGC 5666, DDO 81, VII Zw 330	30819	9.0	0.07	10.33	-17.4	<6.38	-4	in M 81 group
IC 4662, ESO 102-G14, IRAS 17422-6437	60851	10.0	0.28	11.29	-17.2	7.14	336	
Mrk 36, MCG +05-26-046, Haro 4	33486		0.00	15.69	-14.0	<7.64	672	BCDG
Mrk 116A, I Zw 18a, KUG 0930+554	27182		0.02	15.60	-14.5	—	770	in pair, BCDG
Mrk 170, UGC 6448, MCG +11-14-025	35213	99.0	0.00	14.90	-15.7	<7.66	991	pec, BCDG
Mrk 209, Haro 29, I Zw 36, MCG +08-23-035	40665		0.00	14.94	-13.1	—	305	
Mrk 600, MCG +01-08-008	10813		0.19	15.19	-15.6	—	975	in system
NGC 1140, Mrk 1063, MCG -02-08-019	10966	10.0	0.11	12.56	-19.0	8.15	1498	
NGC 2366/63, UGC 3851, Mrk 71	21102	10.0	0.17	11.46	-16.3	<6.72	87	
NGC 3738, UGC 6565, ARP 234	35856	10.0	0.00	11.93	-15.4	<6.48	218	H II
NGC 3991, UGC 6933, Haro 5, MCG +06-26-060 in ARP 313	37613	10.0	0.02	13.32	-19.8	<8.92	3204	in group, BCG
NGC 4214, UGC 7278, IRAS 12131+3636	39225	10.0	0.00	10.14	-17.9	7.63	298	
NGC 4236, UGC 7306	39346	8.0	0.06	10.06	-17.6	6.69	-5	
NGC 4449, UGC 7592, MCG +07-26-009	40973	10.0	0.00	9.94	-17.3	—	211	
NGC 4861, Mrk 59, UGC 8098, ARP 266	44536	9.0	0.01	12.17	-18.0	<7.81	809	BCG
NGC 5398, ESO 384-G32, IRAS 13584-3249	49923	8.1	0.25	12.26	-19.1	<8.11	1227	
UGC 4483, MCG +12-08-048	24213	10.0	0.15	14.72	-17.5:	—	156	
UGC 9560, II Zw 70, Mrk 829, MCG +06-33-004 IRAS 14489+3546	53014	99.0	0.00	14.20	-16.9	<7.81	1213	in pair, pec, BCDG
G_M82 – Non-magellanic irregulars with red spectra								
M 82, NGC 3034, UGC 532, ARP 337	28655	90.0	0.13	9.30	-18.4	9.51	300	disturbed
NGC 5195, UGC 8494, IRAS 13278+4731 in ARP 85	47413	90.0	0.00	10.60	-18.8	8.46	570	in pair

Table 1. (continued)

Group/Object	PGC #	T	A_B mag	B_T mag	M_B mag	$\log\left(\frac{L_{12}}{L_\odot}\right)$	V_R km s^{-1}	Remarks
G_N3448 – Non-magellanic irregulars with blue spectra								
Haro 6, VCC 144, MCG +01-31-030,								
IRAS F12127+0602	39188		0.00	14.90	-17.5	<8.65	2021	H II, pec?
Mrk 1094, II Zw 33, MCG +00-14-010	16868	90.0	0.40	14.00	-19.3	—	2848	
NGC 3077, UGC 5398, IRAS 09592+6858	29146	90.0	0.23	10.71	-17.0	7.46	-16	in M 81 group
NGC 3448, UGC 6024, ARP 205	32643	90.0	0.00	12.48	-18.8	8.56	1388	in pair w/dwarf
G_N3256 – Luminous starbursts with flat spectra								
ESO 103-G35, IRAS 18333-6528	62174		0.32	14.32	-19.6	9.84	3983	
ESO 383-G44, MCG -05-32-052, IRAS 13346-3245	48125	7.0	0.14	13.46	-20.3	9.09	3934	Sd pec, in cluster
IC 2184, Mrk 8, UGC 3852	21123		0.05	13.82	-19.6	8.91	3549	in system, BCG
Mrk 492, IRAS 15566+2657, MCG +05-38-006	56547		0.15	14.56	-19.3	<9.40	4246	
NGC 3256, ESO 263-IG38, VV 65	30785	99.0	0.59	11.90	-21.5	10.25	2781	in cluster, merger
NGC 3994, UGC 6936, ARP 313, ARK 337	37616	0.0	0.02	13.3	-19.8	9.52	3118	pec.? in interaction
NGC 4194, Mrk 201, UGC 7241, ARP 160	39068	10.0	0.00	12.86	-19.8	9.60	2511	BCG, merger
NGC 5635, UGC 9283, IRAS 14263+2737	51706		0.00	12.93	-20.9	9.07	4318	S...
NGC 5695, Mrk 686, UGC 9421	52261		0.00	13.37	-20.4	<9.15	4171	in system?, disturbed Sd
G_N3622 – Luminous starbursts with blue spectra								
NGC 520, UGC 966, ARP 157	5193	99.0	0.05	12.24	-20.0	9.45	2059	merger
NGC 1614, Mrk 617, MCG -01-12-032, ARP 186	15538	5.0	0.23	13.28	-20.9	10.35	4673	in pair, merger
NGC 2684, UGC 4662, IRAS 08514+4921	25024		0.06	13.37	-19.6	<8.99	2878	S...
NGC 3622, UGC 6339, IRAS 11171+6730	34692		0.00	13.20	-18.0	<8.09	1328	S...
NGC 3995, UGC 6944, IRAS 11550+3234								
in ARP 313	37624	9.0	0.02	12.32	-20.9	—	3312	S..., disrupt, in group
NGC 4004, Mrk 432, UGC 6950	37654	99.0	0.00	14.00	-19.3	9.12	3377	SBdm/Im pec, in pair
NGC 5996, Mrk 691, MCG +03-40-039, UGC 10033								
in ARP 72	56023		0.06	12.67	-20.6	—	3297	in pair, distorted SBd
NGC 6052, Mrk 297, UGC 10182, ARP 209	15345	5.0	0.11	13.40	-20.7	9.63	4673	in pair, merger
G_N2782 – Luminous starbursts with very blue spectra								
Mrk 7, VII Zw 153, UGC 3838	21065	99.0	0.08	13.90	-19.2	<8.75	3074	Im, BCG, Pec
Mrk 19, MCG +10-13-071	26180		0.15	15.60	-18.3	<9.07	4200	BCG, in pair
Mrk 25, VII Zw 308, UGC 5408	29177		0.00	14.73	-18.3	<8.80	2985	BCG
Mrk 153, MCG +09-18-032,	32356		0.00	14.43	-18.8	<8.80	3282	BCG, Sc pec, in system
NGC 1741, Mrk 1089, MCG -01-13-045, ARP 259	16574	99.0	0.25	13.80	-20.1	9.10	4004	in system, pec
NGC 2782, UGC 4862, in ARP 215	71554	1.0	0.00	12.01	-20.6	9.51	2532	Sa?
NGC 3690, UGC 6472, IRAS 11257+5850								
in ARP 296	35321	9.0	0.00	11.85	-21.2	10.43	3033	pair/w IC 694, merger
NGC 4670, UGC 7930, Haro 9, ARP 163	42987	0.0	0.04	12.89	-18.0	<8.17	1112	in pair, pec, BCG - H II

spectra effectively used for each galaxy. The spectral group is named after a member which has spectra both in the SWP and LWP/LWR domains with a good (S/N) ratio. The projected IUE aperture in kpc is shown in Table 2 for individual galaxies as well as its average value for the group. The average absolute B magnitude and logarithm of the $12\,\mu$m luminosity (in solar units) are also given in Table 2 for each group. The resulting spectral groups are shown in Fig. 1, with an unprecedented (S/N) ratio in the UV for these galaxy types. Although all these galaxies are enhanced star-formers, there are noticeable differences in terms of spectral features and continuum distributions among them,

suggesting that we are dealing with a range of star formation histories.

4. Measurements

In Paper I we defined a series of windows and regions in the UV which are suitable for measuring equivalent widths (EW) and continuum points in a variety of objects. In Table 3 we present EWs for the UV windows measured in the present spectral groups. The number and wavelength limits of the UV windows (as defined in Paper I), together with the main absorbers in each window, are recalled in the first three columns of Table 3,

Table 2. Nearby star-forming galaxy groups

Galaxy	SWP	LWP/R	slit (kpc × kpc)
G_N1313 – Sm/Im and H II *galaxies with blue spectra*			
$\langle M_B \rangle = -17.1 \pm 1.6$ $\left\langle \log\left(\frac{L_{12}}{L_\odot}\right)\right\rangle \leq 7.43 \pm 0.71$			
			$\langle 0.50 \times 1.00 \rangle$
ESO 435-IG20	1	—	0.80 × 1.60
IC 3017	2	—	1.23 × 2.46
Mrk 33	1	2	0.87 × 1.74
Mrk 67	2	—	0.70 × 1.40
Mrk 450	2	2	0.52 × 1.04
Mrk 487	1	—	0.41 × 0.82
NGC 625	2	2	0.25 × 0.50
NGC 1313	2	2	0.29 × 0.58
NGC 1569	6	4	0.05 × 0.10
NGC 1800	2	—	0.48 × 0.96
NGC 2537	4	—	0.29 × 0.58
NGC 3353	1	1	0.61 × 1.22
NGC 3396	1	—	1.07 × 2.14
NGC 3432	1	—	0.41 × 0.82
NGC 5204	1	—	0.24 × 0.48
NGC 5474	1	1	0.34 × 0.68
NGC 6822	7	3	0.03 × 0.06
NGC 7250	2	1	0.67 × 1.34
UGC 6456	1	—	0.31 × 0.62
UGC 8315N	1	—	0.77 × 1.54
G_N4449 – Sm/Im and H II *galaxies with very blue spectra*			
$\langle M_B \rangle = -16.7 \pm 1.6$ $\left\langle \log\left(\frac{L_{12}}{L_\odot}\right)\right\rangle \leq 7.28 \pm 0.89$			
			$\langle 0.54 \times 1.08 \rangle$
Holmberg II	1	1	0.16 × 0.32
IC 1613	4	2	0.05 × 0.10
IC 2458	1	1	0.94 × 1.88
IC 2574	1	1	0.17 × 0.34
IC 4662	2	1	0.21 × 0.42
Mrk 36	2	—	0.42 × 0.84
Mrk 116A	8	6	0.51 × 1.02
Mrk 170	2	—	0.64 × 1.28
Mrk 209	2	1	0.20 × 0.40
Mrk 600	1	—	0.64 × 1.28
NGC 1140	2	—	0.95 × 1.90
NGC 2366/63	8	3	0.16 × 0.32
NGC 3738	2	1	0.14 × 0.28
NGC 3991	3	1	2.04 × 4.08
NGC 4214	7	1	0.20 × 0.40
NGC 4236	4	1	0.16 × 0.32
NGC 4449	35	15	0.14 × 0.28
NGC 4861	3	3	0.52 × 1.04
NGC 5398	2	1	0.81 × 1.62
UGC 4483	3	0	1.26 × 2.52
UGC 9560	2	1	0.80 × 1.60

Notes: Columns 2 and 3 give the number of IUE spectra effectively used; column 4 gives the projected IUE aperture ($10'' \times 20''$) in kpc × kpc. The average $12\,\mu$m luminosity for each group are calculated from values in Table 1 adopting upper limits in the average.

Table 2. (continued)

Galaxy	SWP	LWP/R	slit (kpc × kpc)
G_M82 – Non-magellanic irregulars with red spectra			
$\langle M_B \rangle = -18.6 \pm 0.3$ $\left\langle \log\left(\frac{L_{12}}{L_\odot}\right)\right\rangle \leq 8.98 \pm 0.74$			
			$\langle 0.26 \times 0.52 \rangle$
M82	4	5	0.16 × 0.32
NGC 5195	1	1	0.37 × 0.74
G_N3448 – Non-magellanic irregulars with blue spectra			
$\langle M_B \rangle = -18.1 \pm 1.1$ $\left\langle \log\left(\frac{L_{12}}{L_\odot}\right)\right\rangle \leq 8.22 \pm 0.66$			
			$\langle 1.04 \times 2.08 \rangle$
Haro 6	1	—	1.31 × 2.62
Mrk 1094	1	—	1.84 × 3.68
NGC 3077	1	—	0.15 × 0.30
NGC 3448	1	1	0.87 × 1.74
G_N3256 – Luminous starbursts with flat spectra			
$\langle M_B \rangle = -20.1 \pm 0.7$ $\left\langle \log\left(\frac{L_{12}}{L_\odot}\right)\right\rangle \leq 9.42 \pm 0.43$			
			$\langle 2.35 \times 4.70 \rangle$
ESO 103-G35	—	1	2.55 × 5.10
ESO 383-G44	1	1	2.57 × 5.14
IC 2184	1	1	2.29 × 4.58
Mrk 492	1	1	2.68 × 5.36
NGC 3256	2	1	1.77 × 3.54
NGC 3994	1	1	2.02 × 4.04
NGC 4194	1	1	1.65 × 3.30
NGC 5635	1	—	2.83 × 5.66
NGC 5695	3	1	2.75 × 5.50
G_N3622 – Luminous starbursts with blue spectra			
$\langle M_B \rangle = -20.0 \pm 1.0$ $\left\langle \log\left(\frac{L_{12}}{L_\odot}\right)\right\rangle \leq 9.27 \pm 0.75$			
			$\langle 2.07 \times 4.14 \rangle$
NGC 520	1	—	1.33 × 2.66
NGC 1614	4	—	2.99 × 5.98
NGC 2684	1	1	1.85 × 3.70
NGC 3622	2	1	0.84 × 1.68
NGC 3995	1	1	2.14 × 4.28
NGC 4004	1	—	2.22 × 4.44
NGC 5996	1	1	2.13 × 4.26
NGC 6052	3	1	3.05 × 6.10
G_N2782 – Luminous starbursts with very blue spectra			
$\langle M_B \rangle = -19.3 \pm 1.2$ $\left\langle \log\left(\frac{L_{12}}{L_\odot}\right)\right\rangle \leq 9.08 \pm 0.66$			
			$\langle 1.96 \times 3.92 \rangle$
Mrk 7	1	1	1.95 × 3.90
Mrk 19	1	—	2.73 × 5.46
Mrk 25	1	1	1.96 × 3.92
Mrk 153	1	—	2.15 × 4.30
NGC 1741	1	—	2.60 × 5.20
NGC 2782	2	3	1.61 × 3.22
NGC 3690	5	3	1.98 × 3.96
NGC 4670	2	1	0.72 × 1.44

respectively. Continuum points, normalised at the corresponding value at $\lambda 2646$ Å, are also provided.

In addition to the galaxy groups of Sect. 2, we also discuss the stellar population of some low-luminosity star-forming early-type galaxies from Paper II which are NGC 5253 and those in the galaxy group G_N1510. These objects are relevant to the present discussion particularly in their comparison with low-luminosity irregular galaxies.

4.1. Relations with global properties

Before analysing in detail the stellar population properties, the high (S/N) ratio templates obtained allow us to test the equivalent widths of some spectral features against the absolute magnitude. We use the lines Mg II, C IV and Si IV, from Table 3. We also use the average $12\,\mu$m luminosity for the groups (Table 2). As expected, there is a strong correlation of $L_{12\mu\mathrm{m}}$ with M_B, since more luminous galaxies contain more metals and consequently more dust too. Among the UV lines, C IV is the one best correlated with absolute magnitude, which suggests that it is a good metallicity indicator for this kind of stellar population. Evidence of this was also found for the star-forming spiral groups in Paper III.

5. Stellar population synthesis

Stellar population synthesis is better constrained when one considers a wavelength range as wide as possible, as emphasised already by e.g. , Bica (1988) and Alloin & Bica (1990). As shown in Paper III for spiral galaxies, synthesis in the UV range is very constrained because of the marked variety of spectral features and continuum distribution occurring in the star cluster components in the UV range, which are predominantly age dependent (Paper I). For this reason, the simplest approach is to perform an independent population synthesis in the UV range alone, and apply the same method to all groups.

Following Bica (1988) and Schmitt et al. (1996), we have adapted the population synthesis algorithm to the UV range in Paper III. Basically this algorithm uses EWs of the most prominent absorption features and selected continuum points observed in a given spectrum, and compares them to those of a model computed from a base of simple stellar population elements. The algorithm is not a simple minimisation procedure, instead it generates all combinations of the base elements according to a given flux contribution step and compares the resulting EWs and continuum points to the input ones. The code successively de-reddens galaxy input continuum points and tests them against a given base model. The acceptable solutions, within error bars, are averaged out: this average is adopted as the final synthesis solution.

The base elements that we use in the present UV synthesis are taken from the star cluster population templates described in Paper I to represent young (including an H II region template) and intermediate age components, and a galaxy template taken to represent an old metal-rich bulge (Paper II). EWs and continuum points of the H II region element were measured on the av-

erage spectrum of the M 101, M 33, LMC and SMC groups from Paper I. For young and intermediate age elements, we use LMC star cluster groups with ages $\approx 10, 25, 75, 200$ and $1200\,\mathrm{Myr}$ (respectively the groups I, II, III, IVA and V in Paper I). Finally, we use a bulge template (named E2E5 by Bica and collaborators – see the database in Leitherer et al. 1996), which is the average of the far-UV weak elliptical galaxy groups G_N1553 and G_N3115 (Paper II). EWs and continuum points for these base elements are listed in Table 8 of Paper III.

All synthesis runs included the 7 age components described above. Initially, we used a 5% step for testing flux contributions at $\lambda 2646$ Å, generating 230 230 combinations for each assumed $E(B-V)$. Typically, for the appropriate $E(B-V)$, only 5% of these 230 230 element combinations are acceptable solutions within the error windows. Reddenings were tested in the range $0.0 < E(B-V) < 0.5$ with a step of $\Delta E(B-V) = 0.01$. Thus, in total, $\approx 1.15 \times 10^7$ element combinations are tested for each group, and acceptable solutions amount to less than 1%. Finally, after probing as above the space of combinations, we calculate the final solution with finer steps of 2% for flux contributions.

The Galactic (Seaton 1979), LMC (Fitzpatrick 1986) and SMC (Prévot et al. 1994) reddening laws have been tested in the synthesis of each group.

Synthesis results for the present irregular galaxy groups, as well as the early-type ones NGC 5253 and G_N1510, are given in Table 4 where we present the percentage contribution of each base element to the group stellar population, with respect to the flux at $\lambda 2646$ Å; $E(B-V)$ values are also given in the table, and they correspond to the SMC law. It is interesting to point out that in no case Seaton's Galactic reddening law can describe these external galaxies, such a correction producing prohibitive high flux excesses in the region around $\lambda 2200$ Å. A similar result has been found for the sample of normal nearby spirals in which there are cases where an SMC reddening law applies and cases where an LMC law applies (Paper III). The same conclusion was reached by Kinney et al. (1994).

Extragalactic reddening laws for extended objects seem to work differently than interstellar ones deduced from stars (Calzetti, Kinney & Storchi-Bergmann 1994), so that the term attenuation is often used now in place of extinction when referring to the loss of light in a galaxy spectrum due to the intervention by dust mixed with the stars. The latter extragalactic obscuration law (EOL) was compared to the LMC and SMC laws (deduced from stars) in Fig. 1 of Calzetti et al. (1995). The EOL on average follows the LMC curve, except that it presents no $\lambda 2200$ Å bump. In this respect it is similar to the SMC curve, which however is steeper. As a consequence, the application of the EOL curve to the present spectra would produce similar results (i.e. SMC law, absence of bump), but the associated colour excesses $E(B-V)$ would be somewhat higher.

The synthesis procedure is illustrated in Fig. 3 for the very blue group of magellanic irregulars G_N4449, which has a dominant flux contribution from the H II region component (Table 4); the spectra are shown in their true proportions (in terms of flux fraction at $\lambda 2646$ Å), according to the synthesis. A similar dis-

Table 3. Equivalent Width and continuum measurements for the galaxy groups

			G_N1313	G_N4449	G_M82	G_N3448	G_N3256	G_N3622	G_N2782
UV#	Window (Å)	Main absorbers				Equivalent Widths (Å)			
4	1290–1318	Si II, Si III	5.55	2.98	14.89	4.10	5.30	7.46	4.50
7	1384–1414	Si IV, Fe V	3.92	3.25	14.88	4.84	6.68	5.74	5.10
13	1534–1570	C IV	5.17	4.01	11.71	5.03	6.08	9.26	4.34
19	1700–1736	N IV, Si IV, Fe IV	1.12	2.06	3.48†	4.95	1.88	1.00	2.49
43	2506–2574	Fe I, Si I, Si III	7.68	4.05	18.64	1.18	12.08	7.58	3.11
44	2574–2596	Mn II, Fe II	5.04	3.29	7.99†	3.57	7.00	5.83	3.94
45	2596–2642	Fe II, Mn II, Si III	4.09	2.52	17.09	2.52	2.66	5.14	2.51
51	2768–2830	Mg II, Mn II, O V	9.34	4.06	17.98	8.52	16.00	8.67	7.73
52	2830–2900	Mg I, C II, Si I	6.13	4.49	12.07	7.46	8.85	4.33	4.08
λ (Å)						Continuum points – C_λ/C_{2646}			
1282			2.92	4.08	1.51	2.28	1.37	2.18	3.09
1348			2.54	3.73	0.78	2.11	1.25	2.11	2.77
1490			2.54	3.39	1.00	2.07	1.41	2.03	2.52
1768			1.88	2.34	0.96	1.75	1.30	1.65	1.99
2079			1.59	1.70	0.98	0.98	1.18	1.33	1.54
2258			1.18	1.39	0.59	0.89	1.07	1.25	1.29
2466			1.15	1.18	0.85	0.90	1.04	1.14	1.10
2959			0.85	0.76	1.55	1.04	1.06	0.99	0.88
3122			0.93	0.70	1.77	1.11	1.07	0.95	0.85

Notes: Uncertainties in EWs are typically $\leq 10\%$; † – Suspected emission line contamination.

Table 4. Stellar population synthesis results

Group	$\lambda 2646$ Å Flux fraction (in%)							$E(B-V)$
Element:	RH II	LMC I	LMC II	LMC III	LMC IVA	LMC V	E2E5	
Age:	2.5 Myr	10 Myr	25 Myr	75 Myr	200 Myr	1.2 Gyr	$\approx$10 Gyr	
G_N1313	25.7	23.9	17.3	10.9	5.7	15.6	0.9	0.02†
G_N4449	58.8	6.9	11.5	16.7	5.7	0.4	0.0	0.00
G_N3256	6.8	14.8	21.2	6.2	17.7	31.4	1.7	0.06†
G_N3622	6.3	45.3	29.2	9.4	5.7	2.4	1.7	0.06†
G_N2782	19.1	40.0	11.6	15.3	10.2	3.1	0.6	0.02†
G_N1510	28.6	44.2	2.0	2.5	4.1	18.8	0.5	0.04†
NGC 5253	47.8	10.2	8.8	13.6	2.7	16.7	0.3	0.03†

Notes: † reddening-corrected using an SMC law.

play in Fig. 4 is related to the starburst group with flat spectrum G_N3256, which presents a considerably different star formation history (an evolved starburst with age $\approx$1–2 Gyr), as denoted by the contributions of the different age components (Table 4).

The ability of the synthesis algorithm to reproduce the observed EWs can be evaluated by the residuals in each absorption feature, which are given in Table 5.

Below we discuss the synthesis results for each group.

5.1. Groups G_N1313 and G_N4449

These groups of magellanic irregulars and H II galaxies are known to be metal deficient from spectroscopic analysis of their emission lines. Indeed, the galaxies NGC 6822 in group

G_N1313, and NGC 4449, Mrk 116A (I Zw 18) and UGC 9560 (II Zw 70) in group G_N4449, encompass oxygen abundances from that of the SMC (or lower) to that of the LMC (Lequeux et al. 1979). Similar results for 5 galaxies in G_N1313 and 2 in G_N4449 are in common with Storchi-Bergmann, Calzetti & Kinney (1994).

The slightly redder spectrum of G_N1313, with respect to G_N4449, is explained in the synthesis (Table 4) by a more uniform distribution of flux contributions among the age components, in particular with an important intermediate /old-age component. The intermediate age population is indeed a substantial contributor in such morphological types, like the LMC (e.g. Bica, Clariá & Dottori 1992; Elson, Gilmore & Santiago 1997).

Table 5. Equivalent Width Residuals

Group	Bulge Fraction (in%)	EW(measured) – EW(synthesis) (in Å)								
		UV#4 Si II	UV#7 Si IV	UV#13 C IV	UV#19 N IV	UV#43 Fe I	UV#44 Mn II	UV#45 Fe II	UV#51 Mg II	UV#52 Mg I
G_N1313	0.9	1.55	−1.10	0.77	−2.64	1.14	−0.30	−0.61	−3.15	0.78
G_N4449	0.0	−0.02	−1.56	−0.70	−1.70	0.11	−1.34	−1.63	−5.19	−0.84
G_N3256	1.7	−0.01	1.36	1.75	−2.80	2.32	0.35	−2.95	0.01	−0.03
G_N3622	1.7	3.27	0.94	5.70	−1.84	2.69	1.80	1.17	−1.85	−1.27
G_N2782	0.6	0.58	0.24	0.27	−0.79	−1.68	−0.25	−1.55	−2.52	−1.45
G_N1510	0.5	1.39	1.15	1.12	−3.25	1.45	−0.58	−2.10	−4.28	0.30
NGC 5253	0.3	0.03	−0.17	−0.05	−1.81	−1.94	0.40	−0.45	−0.07	0.22

Notes: Column 2: percentage bulge fraction with respect to flux at $\lambda2646$ Å.
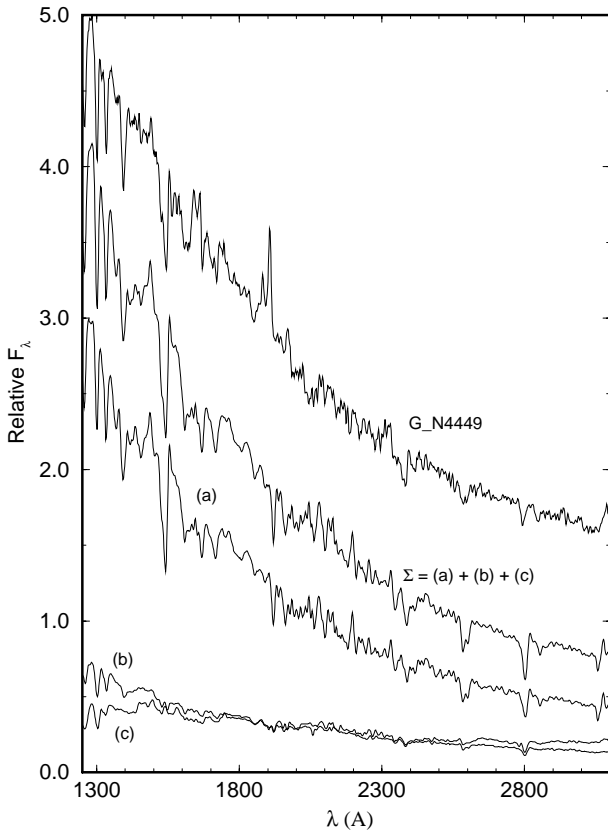
Fig. 3. Stellar population synthesis for the very blue magellanic irregular group G_N4449. (a) H II region template; (b) sum of templates LMC I and LMC II; (c) sum of templates LMC III, LMC IVA and LMC V. A constant has been added to the spectrum of G_N4449 for visualisation purposes. Units as in Fig. 1.

5.2. Groups G_M82 and G_N3448

With regard to metallicity, these groups of non-magellanic irregulars have one galaxy in common with the sample of Storchi-Bergmann et al. (1994), NGC 3077 (in G_N3448). Their oxygen abundance is intermediate between those of the LMC and the Sun.

Interestingly, these intermediate luminosity galaxies are the companions of large spirals, and in some cases, directly inter-
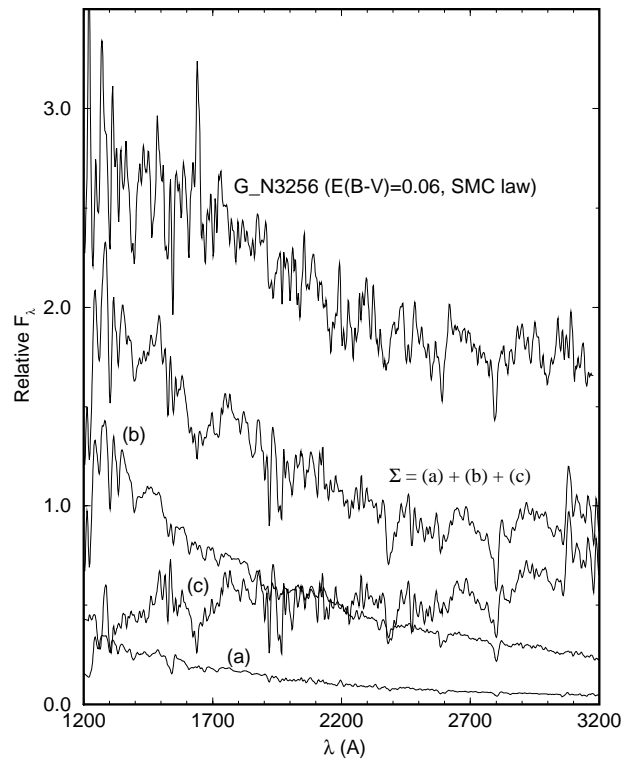

Fig. 4. Stellar population synthesis for the luminous starburst group G_N3256. (a) H II region template; (b) sum of templates LMC I and LMC II; (c) sum of templates LMC III, LMC IVA, LMC V and E2E5. A constant has been added to the spectrum of G_N3256 for visualisation purposes. Units as in Fig. 1.

acting (e.g. NGC 5194 with M 51). The large metallicity of their gaseous component might be explained by accretion of material from the disc of the large spiral.

The rather peculiar and low (S/N) ratio spectra of G_M82 and G_N3448 (Fig. 5) do not allow a detailed synthesis. Instead, we have compared them with the spectrum of the supernova remnant N 49 of the LMC (Paper I). Since the M 82 galaxy is known to contain many supernova remnants (e.g. Unger et al. 1984; Kronberg & Biermann 1983) probably there is a component with this type of spectrum superimposed on its stellar population. This can be seen in particular in the SWP camera

($\lambda\lambda$1200–1900 Å) continuum, and also by the suspected presence of some emission lines, although the low (S/N) ratio precludes any further discussion. The red component in the LWP/R camera range could be accounted for by a bulge or intermediate age contribution. In the group G_N3448 an important flux contribution from young populations seems to be present.

5.3. Group G_N3256

This group is characterised by luminous starbursts with flat UV spectra. This group has objects in common with the sample of mergers by Keel & Wu (1995) which are NGC 3256, NGC 3690 and NGC 4194. they are galaxies in a merging stage where two nuclei are often seen. According to the synthesis (Table 4) no significant bulge flux fraction is detected in the UV. The synthesis results indicate that important star formation occurred both at intermediate (1–2 Gyr) and young ages. The scenario resulting from the synthesis is consistent with a typical time scale for the merging of ≈ 1 Gyr, during which most of the mass has been converted into stars (see Sect. 5.6 and Table 7). The intermediate age component might be identified with the intense star formation in the early interaction and/or the old disk from the spirals. The fact that in the UV the old population is not detected can be explained by dust obscuration in such metal-rich environments, which have essentially solar metallicity, as deduced from oxygen abundances for NGC 3256 and NGC 4194, which are in common with Storchi-Bergmann et al. (1994). We point out that the reddening inferred from the stellar population in the UV is relatively small ($E(B-V) = 0.06$, Table 4), which implies that in the UV we sample stellar populations from more external regions, so that any bulge would be hidden. Indeed, such a large amount of dust is present as denoted by $10\,\mu$m dust emission; for example NGC 3256 and NGC 4194 were studied by Wright et al. (1988). This can also be seen in the $12\,\mu$m IRAS luminosities for individual galaxies (Table 1) and averages for the current groups (Table 2).

5.4. Groups G_N3622 and G_N2782

These groups correspond to starburst galaxies with blue and moderately blue continua. Together with the starburst group with flat spectrum G_N3256, G_N3622 and G_N2782 are luminous both in the optical and at $12\,\mu$m (Table 2). The population syntheses (Table 4) show that G_N3622 is dominated by a slightly evolved burst (10–30 Myr) while G_N2782 is dominated by on-going ($t < 10$ Myr) star formation and a somewhat evolved population ($t \approx 10$ Myr). This difference explains their blue spectra as compared to the flat starburst spectrum of G_N3256, which is dominated by an intermediate age burst (Sect. 5.3). The present stellar population analysis may provide clues to the dynamical age of the interactions.

The important contribution from the H II region component to the group G_N2782 (Table 4) is consistent with the recent HST detailed imaging and spectroscopy of one of the galaxy members, NGC 1741, which revealed two main starbursts, each
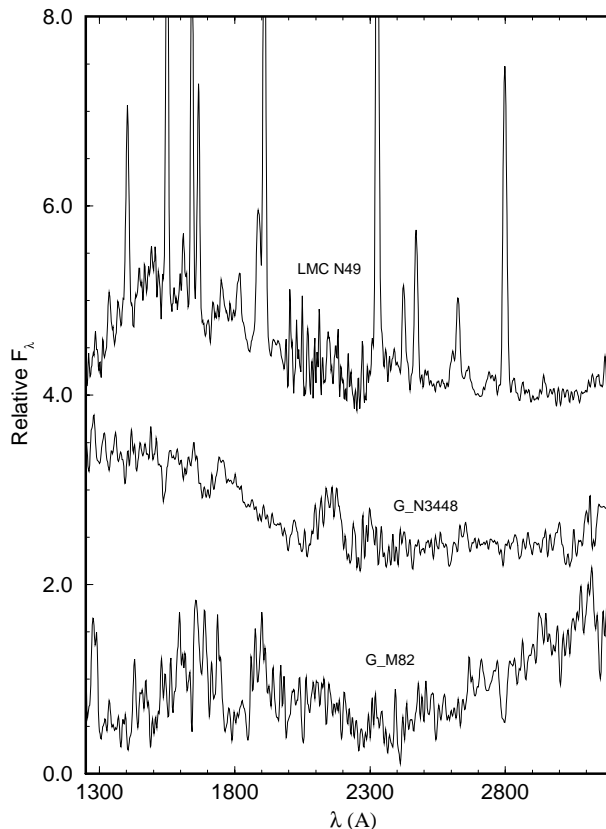

Fig. 5. The peculiar spectra of groups G_N3348 and G_M82 are compared to that of the supernova remnant N 49 in the LMC. Units as in Fig. 1.

being about 100 times as luminous as 30 Doradus (Conti, Leitherer & Vacca 1996).

5.5. Early-type groups G_N1510 and NGC 5253

The galaxies in these groups are classified as early-type in RC3 and a preliminary analysis of their spectral properties were given in Paper II. The population syntheses performed in the present study (Table 4) quantify these early results. The intermediate age population turned out to be important in the UV for both groups, and could be interpreted as the accumulation of earlier star-forming events, probably characterizing the early-type appearance of such galaxies. In Paper II (Fig. 4) the SWP spectrum of NGC 5253 presented absorption features characteristic of H II regions, which was not the case of G_N1510. In fact, the population synthesis confirms this scenario (Table 4). We have included these early-type galaxies in the present analysis to compare them with the magellanic irregular and H II galaxy groups G_N1313 and G_N4449, at comparable optical luminosities. The major difference is the enhanced intermediate age component in the early-type groups.

It can be inferred that the star formation history, and consequently the relative flux contributions of different age components, are related to the morphological appearance and resulting classification of galaxies.

Table 6. Mass to light ratios

Component	Age interval (10^9 yr)	$\frac{M}{L_{5870}}$	$\frac{L_{5870}}{L_{2646}}$	$\frac{M}{L_{2646}}$
R H II	0.0–0.007	0.035	0.14	0.005
LMC I	0.007–0.02	0.007	0.28	0.002
LMC II	0.02–0.07	0.063	0.41	0.026
LMC III	0.07–0.2	0.305	0.65	0.198
LMC IVA	0.2–0.7	0.343	1.60	0.548
LMC V	0.7–7.0	2.270	3.00	6.820
E 2 E 5	7.0–17.0	8.260	19.10	157.7

5.6. Synthesis results in terms of mass

Similarly to what has been done for normal spiral groups in Paper III, we can convert the flux fractions derived from the synthesis into mass fractions. Previous synthesis results in the visible/near-infrared ranges (Bica 1988) have been converted to mass fractions by means of mass to light ratios M/L_V computed from a stellar evolution model of star clusters (Bica, Arimoto & Alloin 1988). Applying these results, we recall in Table 6, for each age component used in the present paper, the corresponding age interval and mass to light ratio expressed in luminosity at $\lambda 5870$ Å. Using our $1\,000$–$10\,000$ Å stellar population templates we measured the ratio L_{5870}/L_{2646}, and derived the mass to light ratio M/L_{2646}, respectively shown in columns 4 and 5 of Table 6.

Mass fractions for the galaxy groups can be obtained from the synthesis flux fractions by means of M/L_{2646}. The results are shown in Table 7. In terms of mass fractions, the old stellar population is dominant in several groups, despite the fact that the UV light is dominated by recent star formation. Some groups have important mass fractions stored at intermediate ages, as a result of the old disk contribution and/or evolved starbursts associated to interactions. In terms of flux, the UV light of the low-luminosity early-type groups G_N1510 and NGC 5253 is dominated by the young components but with important contributions from the intermediate age component. As a consequence, the young components store a negligible mass fraction, the intermediate age stores $\approx 2/3$ while the remaining mass is stored in the bulge. Finally, the bluest group G_N4449, which is flux dominated by the H II region component, is characterised by having $\approx 70\%$ of its mass stored in the young ($t < 500$ Myr) components, with the old disk storing the remaining $\approx 30\%$.

6. Emission lines

Despite the strong absorptions, several emission lines can be clearly seen in our group spectra (Figs. 1, 3 and 4) which are not present in integrated UV spectra of H II regions (see Paper I). To better visualize these lines we have produced one average spectrum with the magellanic irregulars and another for the luminous starbursts. These 2 average spectra are shown in Fig. 6 together with that of the supernova remnant N 49 in the LMC for comparison. Conspicuous in the magellanic irregulars are the semi-forbidden lines O III]$_{\lambda 1658-1666}$, N III]$_{\lambda 1647-1754}$,
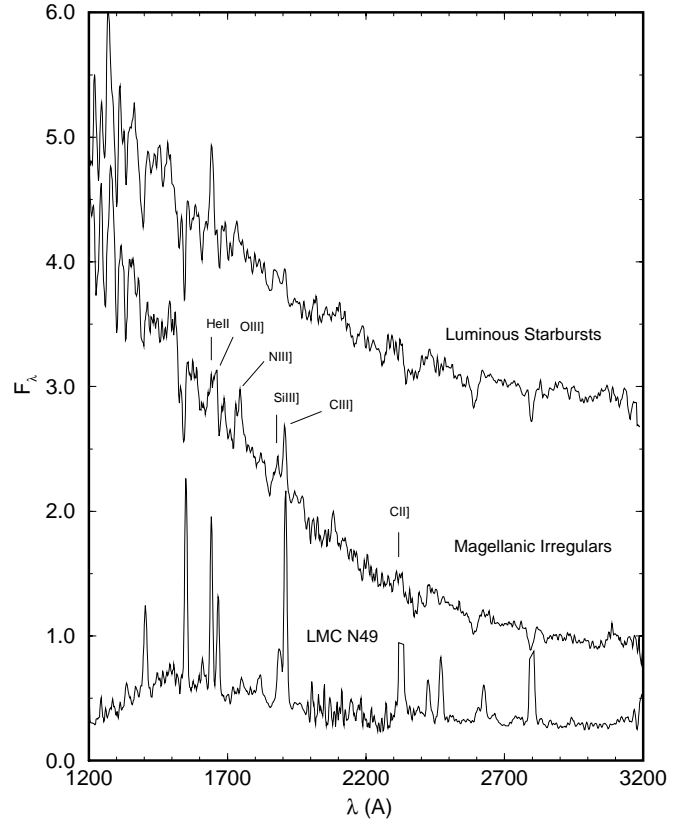

Fig. 6. The average spectra of the luminous starbursts and magellanic irregular groups are compared to that of the supernova remnant N 49 in the LMC. The presence of several semi-forbidden emission lines in the spectrum of the magellanic irregulars suggests they originate from shock-heating. Photoionisation by very hot stars or a low-luminosity AGN may apply to the luminous starbursts. Units as in Fig. 1.

Si III]$_{\lambda 1682,92}$, C III]$_{\lambda 1907,09}$ and C II]$_{\lambda 2325-2329}$, typical of supernova remnants, as well as the permitted line He II$_{\lambda 1640}$. On the other hand, the only conspicuous line in the luminous starbursts is He II$_{\lambda 1640}$, whereas the semi-forbidden lines listed above seem to be present although at a very low level.

The emission-line spectrum of the magellanic irregulars resembles that of the supernova remnant N 49 in the LMC, and it probably originates from shocked gas (Sutherland, Bicknell & Dopita 1993) in supernova remnants and/or winds throughout these on-going star-forming galaxies.

Our groups of luminous starbursts contain mergers, interacting systems, etc., for which shocks are probably an important heating mechanism in the gas. However, since the shock-heated semi-forbidden lines are much less conspicuous in these galaxies than in the magellanic irregulars, and the only strong line is He II$_{\lambda 1640}$, photoionisation by hot stars, not necessarily young, such as post-AGBs (Binette et al. 1994), or even by a low-luminosity AGN seems to be more appropriate.

7. Conclusion

In this paper we have focused our attention on the central, bright parts of nearby star-forming galaxies available in the IUE li-

Table 7. Synthesis results in terms of mass fractions

Group	Mass fraction (in%)						
Element:	RH II	LMC I	LMC II	LMC III	LMC IVA	LMC V	E2E5
Age:	2.5 Myr	10 Myr	25 Myr	75 Myr	200 Myr	1.2 Gyr	≈10 Gyr
G_N1313	0.05	0.02	0.18	0.85	1.23	41.85	55.83
G_N4449	2.94	0.14	2.99	33.02	30.97	29.96	<0.01
G_N3256	0.07	<0.01	0.11	0.25	1.96	43.34	54.26
G_N3622	0.11	0.03	0.26	0.64	1.07	5.63	92.25
G_N2782	0.76	0.06	0.24	2.41	4.45	16.82	75.26
G_N1510	0.07	0.04	0.03	0.24	1.07	61.03	37.53
NGC 5253	0.14	0.01	0.14	1.62	0.89	68.67	28.52

brary. Applying a grouping scheme, we have obtained a series of UV templates with significantly different stellar population contents, as indicated by their population synthesis using as base star cluster template spectra.

The morphological classification of galaxies such as H II, irregular, star-forming low-luminosity early-type, is intimately connected to the star formation history, and the resulting relative flux contribution of each age component. In particular, the detection of intermediate age components in these UV spectra, and the corresponding mass fractions, helps to better explain the formation of subsystems within each galaxy. In this respect we can link the present analysis with the central parts of spiral galaxies whose UV analysis (Paper III) pointed out, in some cases, important mass fractions stored in young and intermediate age components, which might be seen as developing and/or growing bulges. This might explain the different morphologies observed in the central parts of late-type galaxies and the transition to magellanic irregulars (van den Bergh 1995).

We also discuss the luminous starbursts, in particular groups containing mergers which often have the same kind of UV spectrum, i.e. a flat distribution. The population synthesis indicates that important star formation occurred both at intermediate (1–2 Gyr) and young ages.

As pointed out in Paper I, integrated spectra of H II regions in the UV do not contain emission lines. The spectra of our magellanic irregular groups (G_N1313 and G_N4449) do show several semi-forbidden emission lines as well as He II$_{\lambda1640}$ suggesting the presence of shock-heated gas through supernovae explosions. The emission line spectra of the starburst groups (G_N2782, G_N3622 and G_N3256) do not show all these lines and probably originate from photoionisation by very hot stars or a low-luminosity AGN.

As a final remark we emphasize that this link between star formation history and morphology of galaxies in the local Universe, could give an insight into the interpretation of the early Universe, through the observation of high redshift galaxies.

References

Alloin D., Bica E., 1990, RMxAA 21, 182
Bica E., Arimoto N., Alloin D., 1988, A&A 202, 8
Bica E., 1988, A&A 195, 76
Bica E., Clariá J.J., Dottori H., 1992, AJ 103, 1859
Binette L., Magris C., Stasinska G., Bruzual A., 1994, A&A 292, 13
Bonatto C., Bica E., Alloin D., 1995, A&AS 112, 71 (Paper I)
Bonatto C., Bica E., Pastoriza M.G., Alloin D. 1996, A&AS 118, 89 (Paper II)
Bonatto C., Bica E., Pastoriza M.G., Alloin D., 1998, A&A 334, 439 (Paper III)
Calzetti D., Kinney A.L., Storchi-Bergmann T., 1994, ApJ 429, 582
Calzetti D., Bohlin R.C., Kinney A.L., Storchi-Bergmann T., Heckman T.M., 1995, ApJ 443, 136
Conti P.S., Leitherer C., Vacca W.D., 1996, ApJ 461, L87
de Vaucouleurs G., de Vaucouleurs A., Corwin H.G. Jr., et al., 1991, Third Reference Catalogue of Bright Galaxies. Springer-Verlag, New York (RC3)
Elson R.A.W., Gilmore G.F., Santiago B.X., 1997, MNRAS 289, 157
Fitzpatrick E.L., 1986, AJ 92, 1068
Keel W.C., Wu W., 1995, AJ 110, 129
Kinney A.L., Calzetti D., Bica. E., Storchi-Bergmann T., 1994, ApJ 329, 172
Kinney A.L., Bohlin R.C., Calzetti D., Panagia N., Wyse R.F.G., 1993, ApJS 86, 5
Kronberg P., Biermann P., 1983, IAU Symp. 101, 583
Leitherer C., et al., 1996, PASP 108, 996
Lequeux J., Peimbert M., Rayo J.F., Serrano A., Torres-Peimbert S., 1979, A&A 80, 155
Prévot M.L., Lequeux J., Maurice E., Prévot L., Rocca-Volmerange B., 1984, A&A 132, 389
Rosa M., Joubert M., Benvenutti P., 1984, A&AS 57, 361
Schmitt H.R., Bica E., Pastoriza M.G., 1996, MNRAS 278, 965
Seaton M.J., 1979, MNRAS 187, 73p
Sutherland R.S., Bicknell G.V., Dopita M.A., 1993, ApJ 414, 510
Storchi-Bergmann T., Kinney A.L., Challis P., 1995, ApJS 98, 103
Storchi-Bergmann T., Calzetti D., Kinney A.L., 1994, ApJ 429, 1
Unger S.W., Pedlar A., Axon D.J., Wilkinson P.N., Appleton P.N., 1984, MNRAS 211, 783
van den Bergh S., 1995, AJ 110, 613
Wright G.S., Joseph R.D., Robertson N.A., James P.A., Meikle W.P.S., 1988, MNRAS 233, 1